Overview of Power Electronic Converter Topologies Enabling Large-Scale Hydrogen Production via Water Electrolysis

Chen, Mengxing; Chou, Shih-Feng; Blaabjerg, Frede; Davari, Pooya

Published in:
Applied Sciences

DOI (link to publication from Publisher):
10.3390/app12041906

Publication date:
2022

Document Version
Accepted author manuscript, peer reviewed version

Article

Overview of Power Electronic Converter Topologies Enabling Large-Scale Hydrogen Production via Water Electrolysis

Mengxing Chen , Shih-Feng Chou , Frede Blaabjerg and Pooya Davari *

AAU Energy, Aalborg University, Aalborg East 9220, Denmark; mec@energy.aau.dk (M.C.); shih-feng.chou@hitachienergy.com (S.C.); fbl@energy.aau.dk (F.B.); pda@energy.aau.dk (P.D.)
* Correspondence: pda@energy.aau.dk

Abstract: The renewable power-to-hydrogen (P2H) technology is one of the most promising solutions to fulfill the increasing global demand for hydrogen and to buffer the large-scale fluctuating renewable energies. The high-power high-current ac/dc converter plays a crucial role in P2H facilities to transform the medium-voltage (MV) ac power to a large dc current to supply the hydrogen electrolyzers. This work introduces the general requirements and overviews several power converter topologies for P2H systems. The performances of different topologies are evaluated and compared from multiple perspectives. Moreover, the future trend of eliminating the line-frequency transformer (LFT) is discussed. This work can be future guidance designing and implementing of power electronics-based P2H systems.

Keywords: High-power ac/dc converter; IGBT; power-to-hydrogen; water electrolysis; thyristor

Citation: Chen, M.; Chou, S. -F.; Blaabjerg, F; Davari, P. Overview of Power Electronic Converter Topologies Enabling Large-Scale Hydrogen Production via Water Electrolysis. *Journal Not Specified* **2021**, *1*, 0. https://doi.org/

Received:
Accepted:
Published:

1. Introduction

Nowadays, hydrogen is widely used for industry-scale ammonia production for fertilizers and fossil fuel processing (e.g., hydro-cracking). The global demand for pure hydrogen has been rising for recent decades, and it accounted for 74 million tonnes in 2018 [1]. Due to the global ambition to achieve net-zero carbon emission and the transition of using hydrogen-based e-fuels to replace fossil fuels, the future demand for hydrogen is expected to increase by a factor of more than ten in 2050 [2]. However, the mainstream of global hydrogen production is based on steam reforming of natural gas, and this fossil hydrogen production generates CO_2 emission of approximate 830 million tonnes per year [1].

One of the other methods for hydrogen production is water electrolysis, where water is split into hydrogen and oxygen by using electric power [3]. It accounts for 2% of the global hydrogen supply [4]. The water electrolyzer typically consumes 50 kWh electricity power for producing 1 kg of hydrogen. Therefore, the CO_2 emission of hydrogen from water electrolysis is highly dependent on ways of electricity generation. Using coal-based electricity will lead to heavy carbon emissions, whereas renewable power, e.g., wind turbines and photovoltaics, involves no carbon emissions. Hence, this renewable hydrogen production via water electrolysis is promising to fulfill the increasing worldwide hydrogen demand and to achieve net-zero carbon emissions by 2050 [5].

On the other hand, the global warming crisis also led to booming interests and investments in renewable energy over recent decades. As such, a large number of wind farms and photovoltaic power plants are being built worldwide [6]. However, the high penetration level of renewable energies brings a fluctuating nature to the power grid and causes instability issues, as their electricity productions are highly dependent on climate conditions [7]. The power-to-hydrogen (P2H) facilities can act as energy storage units by transforming the excessive energy delivered by renewable sources to hydrogen when low electrical demands are present. The hydrogen storage can be converted back to electricity via fuel cell converters during high electricity demand periods. In both ways, the intermittent nature of renewable power can be balanced to well match the demand profile of power grids [8–10]. Moreover, The generated hydrogen can be utilized as green fuel for mobility as well as raw material in the chemistry industry.

Due to the emission and grid-support features of the renewable hydrogen system, in recent years a booming number of demonstration and commercial plants are newly built worldwide [11–13]. Figure 1 demonstrates the general architecture of the renewable hydrogen system [14]. Renewable energies typically comes from wind turbines and photovoltaic power plants, which are connected to medium-voltage (MV) or high-voltage (HV) ac power grid via the ac/dc/ac frequency converter and dc/ac inverter, respectively. The generated renewable electricity then transmits through power grid to the hydrogen production site. The P2H converter plays a crucial role in this renewable hydrogen plant as it converts the MV ac electricity from the grid to a controlled high-current dc power flow, which is fed into the water electrolyzer for large-scale hydrogen production. The produced hydrogen can be directly used or further converted to methane and methanol, which are widely used in various industries, such as oil refining, mobility, and electricity generation.

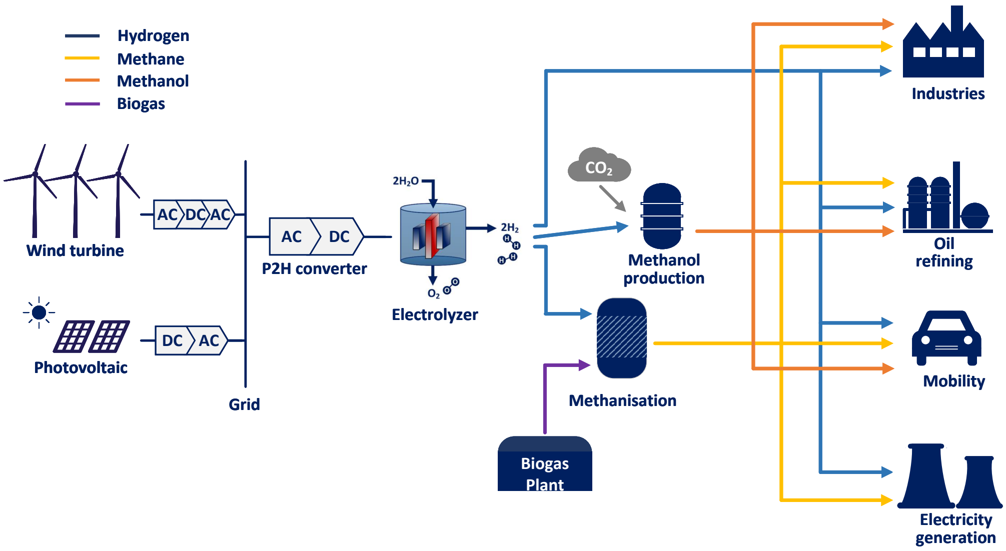

Figure 1. The general architecture of renewable hydrogen system including the renewable energy generation, the distribution and conversion of electricity, the P2H electrolysis, and the application of renewable hydrogen.

The power quality, efficiency, cost, and reliability are several of the P2H system's critical performance metrics, which can be significantly affected by the topology of P2H converters. Thyristor-based ac/dc power converters have been dominating solutions in high-power ac/dc applications due to their high robustness, high efficiency, and low cost [15–22]. A commercial thyristor-based converter can supply 1.5–10 kA dc current with a dc voltage of 1 kV, delivering 10 MW power in maximum per unit [22]. Nevertheless, the large firing angle operation of thyristors can result in heavy current distortion and low power factor at the ac input. Hence passive/active power filters and reactive power compensators are mandatory, increasing the system-level cost [16]. Moreover, a significant trend in recent years is to use Buck-type chopper as the rear stage of diode/thyristor rectifier [20,21,23–28]. A commercial chopper rectifier can supply a maximum of 10.4 kA and 1.1 kV at the dc output, delivering 10 MW power to the electrolyzers [28]. This brings better power quality and higher power factor throughout a wide operation range of the converter. Moreover, the emerging active-front end (AFE) based on the B6 converter can also be an attractive option for the power-to-hydrogen application [29]. It brings much fewer input current distortion by fully regulating the input ac current waveform. In this way, the active/passive power filters and the reactive power compensators can be eliminated.

In the literature, there are some comparative works available. In [19], four thyristor-based ac/dc high-current rectifier topologies are compared, where the chopper-rectifier and AFE solutions are not covered. Reference [20] reviews the thyristor phase-controlled rectifiers, IGBT chopper rectifiers, and pulse-width modulated current source rectifiers for various industry applications requiring kilo-amperes supplies. It is concluded that the IGBT chopper rectifier has had fulfilled field experience to perform as an alternative for supplying kilo-amperes current. Reference [21] overviews the diode- and thyristor-based multi-pulse rectifiers with on-load tap changing transformer as well as the chopper-rectifier topologies. A future research trend on modular converter topologies with medium-frequency transformer (MFT) and high-frequency transformer (HFT) is introduced in [21]. Nevertheless, none of the aforementioned provides an insight into the P2H water electrolysis system. Moreover, the performance matrix of using AFE converter in such P2H water electrolysis system is not investigated in prior-art.

This paper focuses on the P2H water electrolysis system and serves as the overview and comparison of P2H power electronic converter topologies. This paper first introduces the general requirements of P2H converters from both the electrolyzer side and grid side in Section 2. Then, several power converter topologies used in P2H water electrolysis are introduced and studied from multiple perspectives in Section 3. The comparative conclusions regarding the power quality, efficiency, cost, reliability, and control complexity are drawn in Section 4. The future trend of using the modular multi-cell converter to eliminate the bulky line-frequency transformer (LFT) is discussed in Section 5. Finally, the conclusions are drawn in Section 6.

2. General Requirements

2.1. Load Specifications

A simplified electrical model of a hydrogen electrolyzer is exhibited in Figure 2, where U_{rev} and R_Ω are the reverse voltage potential and ohmic resistance during the water-splitting reaction. Furthermore, components C_{dl} and R_{ct} describe the charge transfer resistance and double layer capacity, respectively, which are temperature-dependent. It is noted that R_Ω suffers a parametric increase along with the aging process of the electrolyzer. Thereafter, the loading ranges, i.e., dc current and voltage level, of the hydrogen electrolyzer at its beginning of life (BOL) and end of life (EOL) are presented in Figure 3.

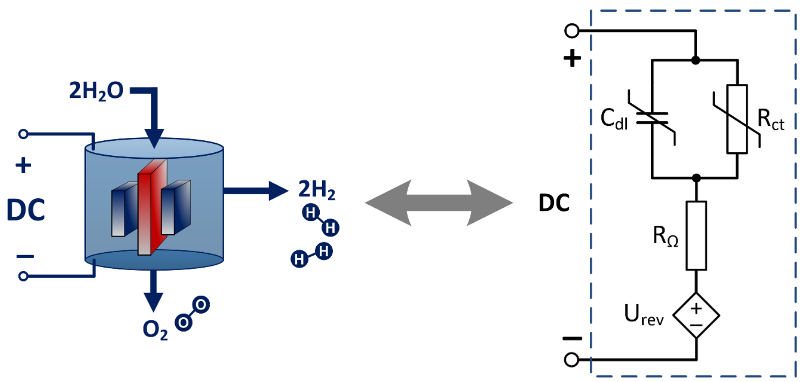

Figure 2. The electrical model of a hydrogen electrolyzer. [30]

According to the electrolyzer's specification, the general requirements of a power-to-hydrogen power converter are listed in Table 1. The output voltage is in the range of 640–1000 V (see Figure 3) due to variations of the current level and electrolyzer degradation. The output power can reach 10 MW using two sets of 5 MW electrolyzer stack, with a rated load current up to 5 kA for each. A future trend of the load specification is to have a current ripple of less than 5%.

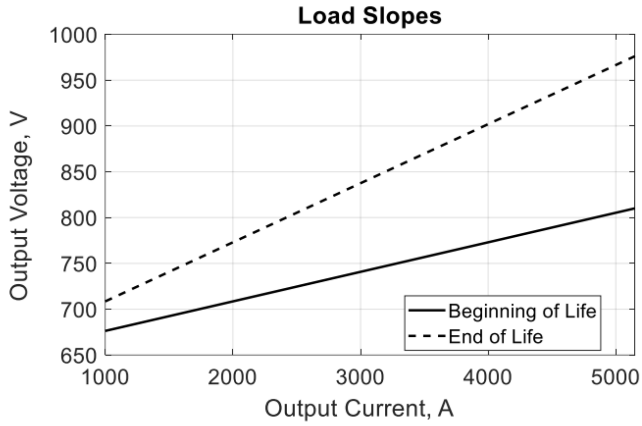

Figure 3. Load slopes of the electrolyzer for the beginning and end of lifetime.

Table 1. General requirements of power-to-hydrogen power converters.

	Present	**Future**
Input voltage	Typical 6.6–35 kV, 50/60 Hz	
Output voltage	640 – 1000 V	
Output power	5 MW × 2 (2 sets of electrolyzer stack, 5 kA each)	
Output current ripple	N/A	$\leq$ 5 % of rated current
Efficiency	$>$ 94 %	$>$ 98 %
Power factor	$>$ 0.90	$>$ 0.99
THD_i (2–40^{th})	$<$ 5 %	
Standards	IEC 60076 series (transformer) IEC 60146-1-1 (semiconductor converter) [31] IEC 61000-6-2 (immunity) [32] IEC 61000-6-4 (emission) [33] IEC 61000-3-6 (distortion) [34] IEC 61000-3-7 (voltage fluctuations) [35] IEC 61000-3-13 (unbalanced installations) [36]	

2.2. Grid Requirements

Typically, the MW-level power-to-hydrogen converter is connected to a MV 6.6–35 kV power grid, where a step-down LFT is mandatory in between. From the grid's perspective, there are several requirements for power-to-hydrogen converters as consumption installations. First, the converter should maintain regular operations under background frequency and voltage deviations, in the range of 47 – 63 Hz and 90% – 110% of the nominal voltage, respectively. Furthermore, the regular operation of power converters should not cause severe power quality issues, e.g., voltage imbalance, rapid voltage change (i.e., 4%), and flickers [35,36]. Moreover, harmonic distortions and interferences in 2 – 9 kHz should be attenuated, according to IEC 61000-3-6 [34]. The current total harmonic distortion (THDi) and power factor at the connection point should be less than 5% and greater than 0.90, respectively. In order to fulfill the electromagnetic compatibility requirements, standards IEC 61000-6-2 [32] and IEC 61000-6-4 [33] apply for P2H power electronic converters.

3. State-of-the-Art Solutions

3.1. 12-Pulse Thyristor Rectifier (12-TR)

The multi-pulse thyristor rectifier is one of the most mature and prominent solutions in high-power rectification applications. The block diagram of a 12-pulse thyristor rectifier (12-TR) is depicted in Figure 4. A three-winding wye-delta-wye LFT is connected to eliminate the 5^{th} and 7^{th} order harmonic currents. Then, two 6-pulse thyristor rectifiers are connected to the two secondary windings of the LFT. The electrolyzer current can be regulated by adjusting the firing angle α_f of the dual thyristor rectifiers. A large firing angle α_f is generally adopted for low-power operating conditions, leading to more harmonic and reactive components. The power factor and total demand distortion are pretty dependent on the firing angle, and a large firing angle leads to a lower power factor and more waveform distortion. Consequently, it is mandatory to compensate for these harmonic currents and reactive power at the connection point. Passive trap filters tuned at 11^{th} and 13^{th} order of line frequency are commonly used for P2H converters based on this 12-TR topology. Moreover, a shunt passive high-pass filter may also be implemented to bypass those high-order current harmonics. Besides, a static VAR compensator or static synchronous compensator shall also be mandatory to provide significant reactive power due to the large-firing-angle operation of 12-TR [16].

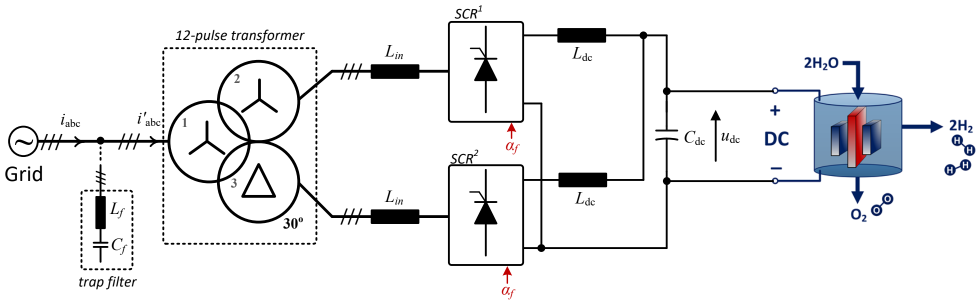

Figure 4. Circuit diagram of a 12-pulse thyristor rectifier with passive trap filter (12-TR).

3.2. 12-Pulse Diode Rectifier with Multi-Phase Chopper (12-DRMC)

Another trendy topology used in P2H power electronic converters is the 12-pulse diode rectifier with multi-phase choppers (12-DRMC) [20,23,24,27], as is illustrated in Figure 5. The multi-phase chopper bridges are implemented by silicon (Si) IGBTs and freewheeling diodes, as arranged in an interleaved manner to attenuate the current ripple through the electrolyzer. The electrolyzer current/power can be regulated by varying the duty ratios of chopper IGBTs. Compared with the 12-TR, one significant merit of the 12-DRMC is the improved power quality, in terms of relatively lower current distortion and constantly high power factor throughout the variable operation range of the P2H converter. Nevertheless, measures are still needed to improve the power quality at the connection point. The widely adopted method involves 11^{th} and 13^{th}-tuned shunt passive trap filters as well as a shunt high-pass filter. Nowadays, the technology of the high-current chopper-rectifier becomes mature [28], and its overall cost decreases as it is presently comparable with the aforementioned 12-TR system [24].

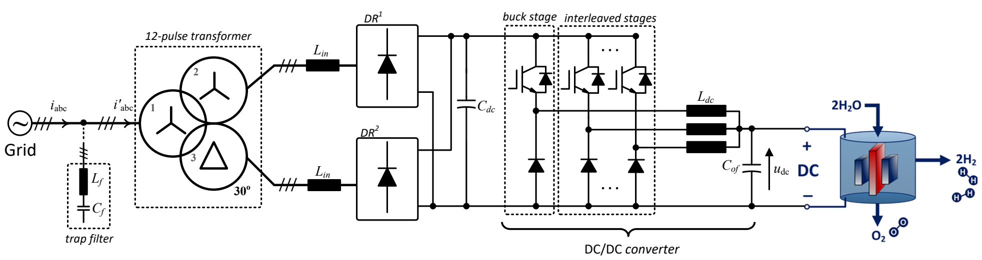

Figure 5. Circuit diagram of a 12-pulse diode rectifier with multi-phase chopper and passive trap filter (12-DRMC).

3.3. 12-Pulse Thyristor Rectifier with Active Shunt Power Filter (12-TRASPF)

Considering the advantages and disadvantages of the above two topologies, a hybrid architecture, a 12-pulse thyristor rectifier with active shunt power filter (12-TRASPF), is proposed [16], as is depicted in Figure 6. The electrolyzer is supplied by the 12-TR, since it features lower costs and high-current capability. The power quality issues of the 12-TR are compensated by a low-power shunt active power filter. Although the loss and cost of the 12-TRASPF system can be more significant compared to 12-TR, promising power quality can be expected.

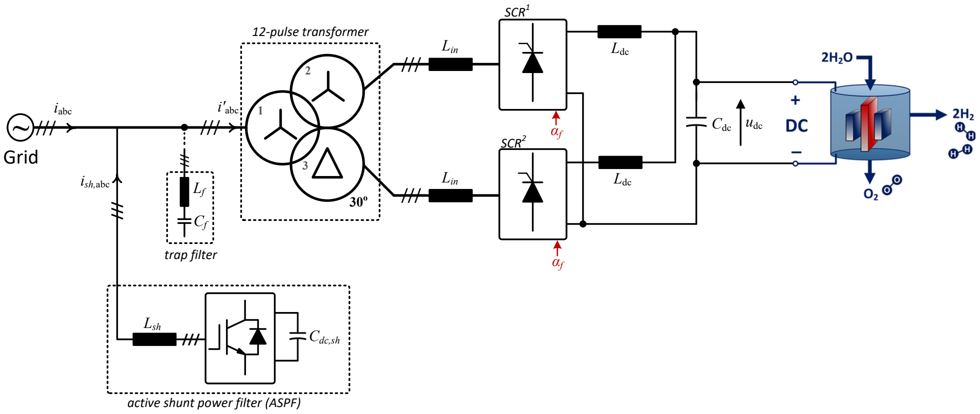

Figure 6. Circuit diagram of a hybrid system with 12-pulse thyristor rectifier and active shunt power filter (12-TRASPF).

3.4. Active Front End (AFE) Rectifier

Another attractive topology candidate is the active front end (AFE) rectifier [29], as is depicted in Figure 7. The popular B6 converter can be utilized, which consists of three IGBT half bridges. Under the case where wide-range operation capability is required, another B6 + chopper architecture may be used to achieve the adjustment of output current and voltage, as depicted in Figure 7 [37]. To simplify, this work focuses on B6-AFE, and conclusions drawn from B6-AFE can also be extended to B6 + chopper-AFE.

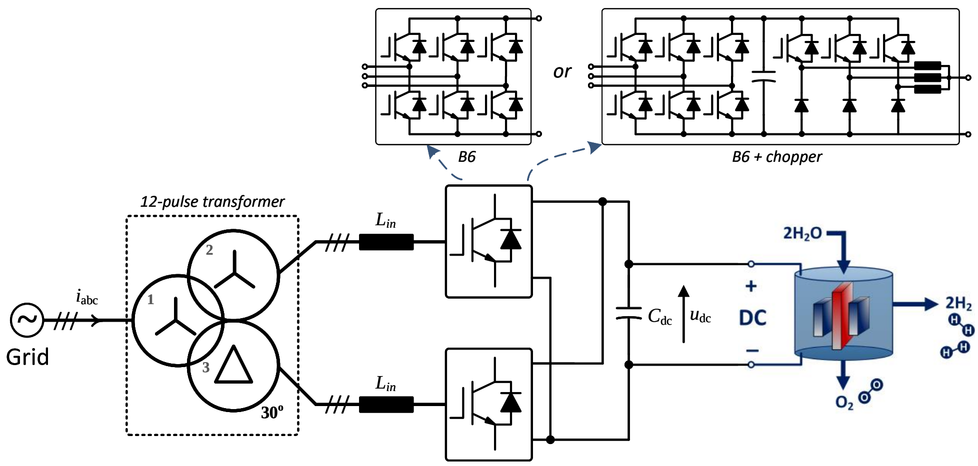

Figure 7. Circuit diagram of an active front end rectifier (AFE).

Due to the current-rating limitation of commercial IGBTs [38], multiple (≥2) IGBT-based B6 converter stacks configured in parallel are mandatory for a power level of 10 MW. Three-winding LFTs used in 12-TR and 12-DRMC can still be employed in AFE systems to achieve the desired power rating, provide galvanic isolation, as well as to mitigate the $6k \pm 1^{th}$ $(k = 1, 3, 5, ...)$ harmonics, although these harmonics are minor components for a B6-AFE system.

In the AFE rectifier system, the input-side ac current can be controlled to be sinusoidal by shaping the duty ratio of the Si IGBTs, so that much lower current harmonic distortion shall be expected for such AFE rectifier systems. Moreover, the phase shift of ac current with respect to grid voltage can also be manipulated by adjusting the modulation signal of the B6 converter so that a high power factor value can be achieved simultaneously. Therefore, one unique advantage of using the AFE rectifier system is its superior power quality regulation capability. No additional passive/active harmonic filters and VAR compensators will be needed.

The AFE rectifier system can also be implemented using the emerging SiC MOSFETs as a substitution of Si IGBTs. The SiC-based AFE rectifiers are demonstrated in [39,40]. One unique feature of the SiC-based B6-AFE rectifier is that the SiC MOSFET can be operated under the synchronous rectification mode by its channel reverse conduction, which features low conduction loss. It is reported in [40] that the AFE rectifier achieves 1.2% efficiency promotion by utilizing 1200-V SiC MOSFETs.

4. Performance Comparison

This work obtains the power factor and current total harmonic distortion (THDi) among 12-TR, 12-DRMC, and 12-TRASPF through simulation. Figures 8 and 9 exhibit the simulated power factor and THDi of the three topology candidates, respectively. It can be seen from Figure 8 that the 12-TRASPF features superior power factor values (≥ 0.99) since the ASPF module can also compensate for reactive power. The 12-DRMC also performs satisfactorily in terms of power factor, i.e., between 0.96 and 0.98, which is relatively flat according to the output variation. For 12-TR based systems, the power factor becomes unsatisfactory under small output-current conditions due to their large firing angles. Therefore, depending on their operating range of output current, the 12-TR requires external power-factor correction measures (e.g., a static VAR compensator, static synchronous compensator, or ASPF module) to compensate for their reactive power. Furthermore, it can be seen from Figure 8 that the power factor of the 12-TR system increases as the electrolyzer becomes more aged, given the identical amount of output current. This can be explained by the increase of electrolyzer resistence alongside its aging process (see Figure 3), leading to the increased portion of active power fed into the electrolyzer given the identical amount of current.

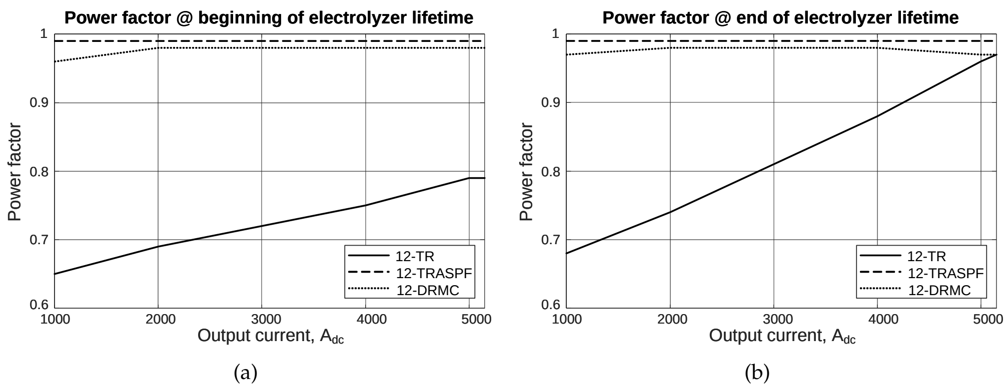

Figure 8. Performance comparison of power factor over the possible operating conditions: (**a**) At the beginning of electrolyzer lifetime. (**b**) At the end of electrolyzer lifetime.

In Figure 9, it is noted that the simulated THDi values of 12-TR and 12-DRMC are obtained without involving any power filters. It turns out that both 12-TR and 12-DRMC will need external passive power filters to attenuate their current harmonic levels, as mentioned in Section 3.1 and 3.2. On the other hand, using the ASPF can also be a promising solution to handle the power quality issue, as the THDi values of 12-TRASPF are well-regulated to be lower than 5%. On the contrary, the AFE rectifier does not seem to have power quality issues as both the phase-lag angle and input current waveform can be well controlled by IGBT-based B6 converters. The power quality rating of the four aforementioned topologies is summarized in Table 2.

Regarding the efficiency performance, the 12-DRMC system exhibits more losses than the 12-TR system. The excessive dissipation of 12-DRMC comes from IGBT's

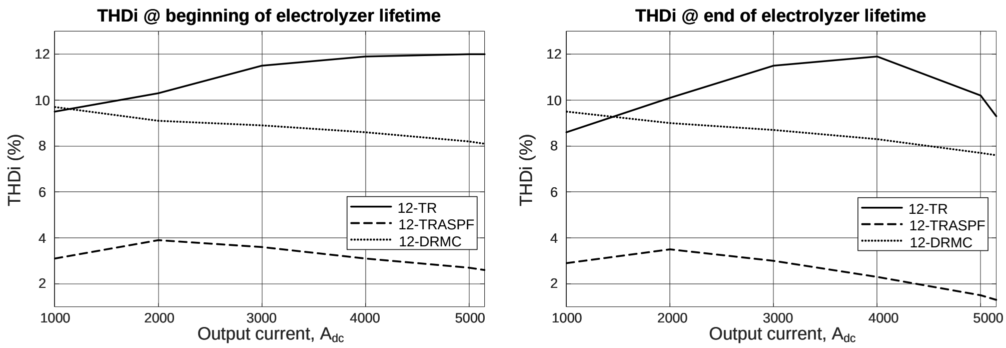

(a) (b)

Figure 9. Performance comparison of THDi over the possible operating conditions: (**a**) At the beginning of electrolyzer lifetime. (**b**) At the end of electrolyzer lifetime.

Table 2. Comparison among topology candidates. ++: Superior. +: Satisfactory. Δ: Neutral. −: Unsatisfactory.

Topologies	Power quality	Efficiency	Cost	Reliability	Control Complexity
12-TR	−	+	+	++	+
12-DRMC	Δ	Δ	+	+	Δ
12-TRASPF	+	Δ	Δ	Δ	−
AFE	++	Δ	−	Δ	−

conduction and switching losses. The percentage of IGBT's switching loss is dependent on its switching frequency and gate driver parameters. The 12-TRASPF system is also less efficient than the 12-TR, considering the extra losses dissipated in the active power filter. From a reliability viewpoint, the 12-TR system exhibits the best performance. The thyristors are considered as reliable components as they have demonstrated their maturity in utility-scale applications. The 12-DRMC is considered less reliable as multiple Si IGBTs are used as the output stage. Nevertheless, the industry is gradually gaining confidence in terms of the reliability of 12-DRMC, as more projects using 12-DRMC are being carried out [20,21]. It is noted that the reliability performance investigated in this work is a system-level concept. For the 12-TRASPF system, a single failure from either the ASPF or 12-TR is regarded as a failure from the system perspective. Although the 12-TR is reliable, the 12-TRASPF system is regarded as neutral in terms of reliability being comparable with the AFE rectifier, because commercial ASPFs use the IGBT-based B6 topology, which is identical with the AFE rectifier presented in this work. The principles of their control and driver systems are also of the comparable level of complexity.

5. Future Trends and Opportunities – Modular Multi-Cell Rectifier

Among the aforementioned P2H converter topologies, the three-winding LFT is mandatory in the system. It is usually the bulkiest component in such a P2H converter system and brings challenges in transportation, installation, and footprint occupation. Therefore, eliminating the bulky LFT from such a P2H converter system is one of the emerging topics.

One promising topology solution is the modular multi-cell rectifier system, as shown in Figure 10. Modular configurations are employed, and each converter cell is implemented by the front-end ac/dc stage followed by a dc/dc stage with galvanic isolation. The highly modularized design enables high scalability and flexibility for the rectifier system. Figure 10(a) demonstrates a star-connected input-series output-parallel (ISOP) configuration to interface with the MV grid [41,42]. Due to the cascaded configuration of converter cells per phase, 1200/1700-V Si IGBT and SiC MOSFET can be used ahead of the dc/dc galvanic isolation in each converter cell [43].

Moreover, a star-connected input-parallel output-parallel (IPOP) configuration is depicted in Figure 10(b). It is noted that the ac side can be configured as either a star or delta connection, and the star type features lower voltage stress for each converter cell [44,45]. When connecting the IPOP type to the MV grid, a single converter cell that interfaces with the MV grid is mandatory, and the 10-kV SiC MOSFET is found to be the significant enabling device [46]. A 25 kW 7 kV/400 V ac/dc converter using 10-kV SiC MOSFETs is successfully demonstrated in [47], and challenges in terms of flashover fault, high switching losses, MV-cable oscillation, and dielectric dissipation are addressed. In the near future, the magnetic components and dielectric materials should be promoted to fully release the potential of this MV SiC-based IPOP-type modular multi-cell converter. Furthermore, the IPOP type makes it compatible when connecting the modular multi-cell rectifier to a low-voltage, e.g., 400 V, power grid using 1200-V voltage-class devices.

The realizations of each ac/dc and dc/dc stages are well established. The single-phase ac/dc stage can be implemented by a full-bridge converter with four active switches, as shown in Figure 10(c). A soft-switching variant with the zero-voltage-switching capability is proposed in [47]. Moreover, it is noted that the three-phase ac/dc stage using a B6 topology is also promising for connecting to LV grids [48]. Under the case where each converter cell is designed to bear high power rating, the three-phase ac/dc gains advantage in terms of a higher efficiency. The dc/dc stage can be realized by multiple converter topologies, such as the dual active bridge [49] (as shown in Figure 10(d)) and LLC converters [50]. Since HFTs/MFTs are to be used in the dc/dc stage, each converter cell can be achieved with a small volume and lightweight. Compared to Si IGBTs, Si and SiC MOSFETs are better choices for each dc/dc stage, as a higher MFT/HFT alternating frequency can be easily achieved. Nevertheless, the highly modularized design also brings high control complexity to the system. Each modular converter cell needs to be able to regulate itself and equally share the operating power.

6. Conclusion

This work provides as an overview of high-power, high-current ac/dc converters for P2H water electrolysis applications. The general load specification (for water electrolyzer) and electricity grid requirements are introduced first to help guide the selection of the P2H converter topologies. Then, four state-of-the-art solutions, i.e., 12-TR, 12-DRMC, 12-TRASPF, and AFE rectifier, are reviewed in this work. Then, these four different topologies are evaluated and compared from various perspectives, including power quality, efficiency, cost, reliability, and control complexity.

The conventional 12-TR is characterized as superior in terms of efficiency, cost, reliability, and control complexity, whereas power quality issues (both power factor and current distortion) need to be addressed, especially under large firing-angle conditions. The 12-DRMC exhibits a high power factor among full operation range compared to 12-TR, while the harmonic filter is still needed to lower its input THDi. The 12-TRASPF is hybrid concept utilizing both conventional 12-TR and a B6 converter based active shunt power filter, so that promising power quality can be expected with a bit more cost and less efficiency compared to 12-TR. The AFE rectifier is a promising solution in terms of superior power quality with no additional compensation measure. Nevertheless, it may suffer from a higher cost as well as a more sophisticated control system.

However, the four aforementioned topologies all require a LFT, which is bulky and with a large footprint occupation. Then, a future trend of eliminating the LFT from the P2H converter is introduced in this work. A modular multi-cell converter is discussed in detail in this work, which gives an interesting research prospective in the near future.

Funding: This research was funded by Energy Technology Development and Demonstration Program (EUDP) under grant 64019-0014.

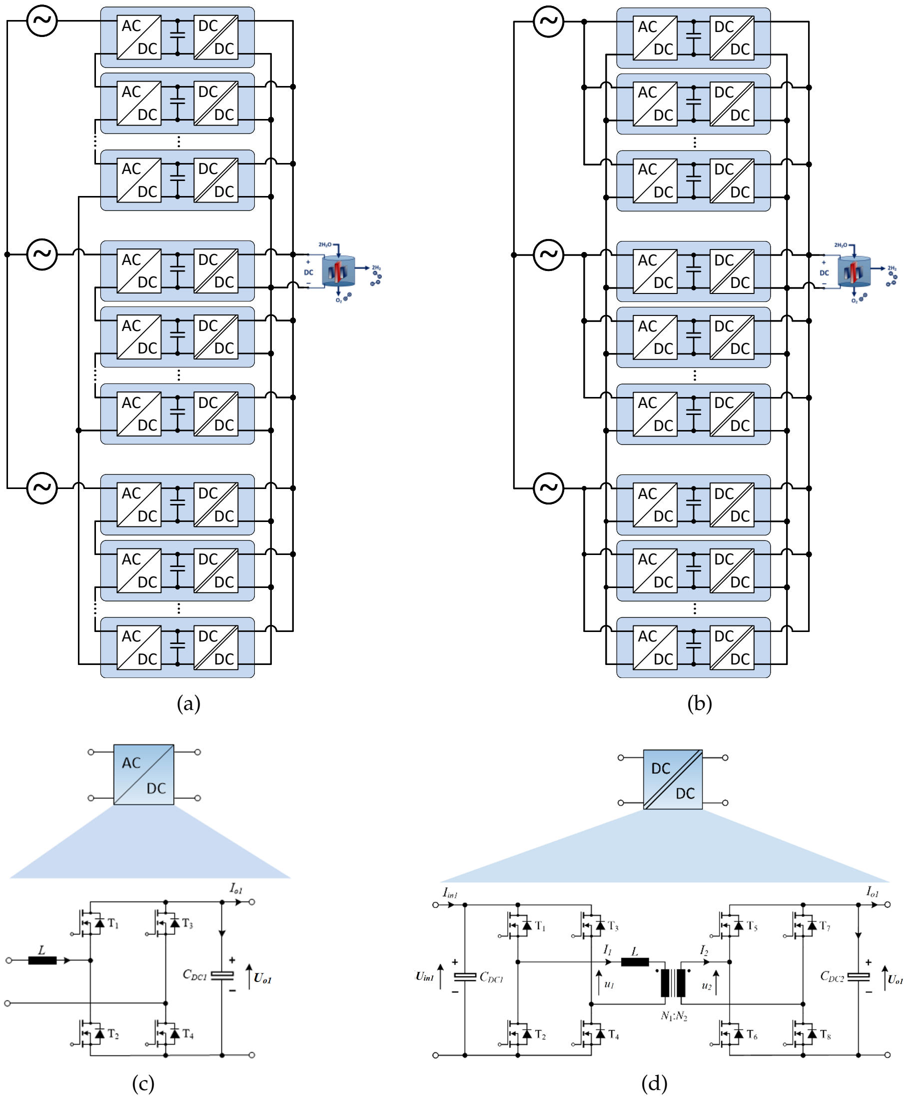

Figure 10. Circuit diagram of modular multi-cell rectifier. (**a**) The circuit architecture in a star-connected ISOP configuration. (**b**) The circuit architecture in a star-connected IPOP configuration. (**c**) The ac/dc stage realized by a single-phase full-bridge circuit. (**d**) The dc/dc stage realized by a dual active bridge circuit.

References

1. The future of hydrogen, Technology report, IEA , Jun. 2019. Available online: https://www.iea.org/reports/the-future-of-hydrogen (accessed on 4^{th} Dec. 2021).
2. Making mission possible: delivering a net-zero economy, Technology report, Energy Transitions Commission, Sept. 2020. Available online: https://www.energy-transitions.org/publications/making-mission-possible/ (accessed on 4^{th} Dec. 2021).
3. Ursua, A.; Gandia, L. M.; Sanchis, P. Hydrogen production from water electrolysis: current status and future trends. *Proceedings of the IEEE* **2012**, *100*, 410–426. doi: 10.1109/JPROC.2011.2156750.
4. The “renewable molecule”: The potential of hydrogen from renewable energy, white paper, Orsted. Available online: https://orsted.com/en/about-us/whitepapers/decarbonising-society-with-power-to-x/power-to-x.
5. A hydrogen strategy for a climate-neutral Europe, white paper, European Commission, Jul. 2020.
6. Blaabjerg, F.; Teodorescu, R.; Liserre, M.; Timbus, A.V. Overview of Control and Grid Synchronization for Distributed Power Generation Systems. *IEEE Trans. Ind. Electron.* **2006**, *53*, 1398–1409.
7. Koutroulis, E.; Kalaitzakis, K. Design of a maximum power tracking system for wind-energy-conversion applications. *IEEE Trans. Ind. Electron.* **2006**, *53*, 486–494.

8. Santos, D.M.F.; Sequeira, C.A.C.; Figueiredo, J.L. Hydrogen production by alkaline water electrolysis. *Química Nova* **2013**, *36*, 1176–1193.
9. Carmo, M.; Fritz, D.L.; Mergel, J.; Stolten, D. A comprehensive review on PEM water electrolysis. *International Journal of Hydrogen Energy* **2013**, *38*, 4901–4934.
10. Wind resource: utilising hydrogen buffering – electrolyser. Available online: http://www.esru.strath.ac.uk/EandE/Web_sites/08-09/Hydrogen_Buffering/Website%20Electrolyser.html (accessed on 11th Oct. 2021).
11. Shell starts up hydrogen electrolyser in China with 20 MW production capacity, Shell plc. Available online: https://www.shell.com /media/news-and-media-releases/2022/shell-starts-up-hydrogen-electrolyser-in-china-with-20mw-product.html (assessed on 30th Jan. 2022).
12. From wind power to green hydrogen. Available online: https://hybalance.eu/ (assessed on 30th Jan. 2022).
13. Linde engineering to build 24 MW PEM electrolyzer plant for Yara, Linde plc. Available online: https://www.linde-engineering.com/en/news_and_media/press_releases/news20220128.html (assessed on 30th Jan. 2022).
14. Blaabjerg, F., Ten breakthrough ideas in energy for the next ten years: power to e-fuel, Global Energy, 2021.
15. Siebert, A.; Troedson, A.; Ebner, S. AC to DC power conversion now and in the future. *IEEE Trans. Ind. Appl.* **2002**, *38*, 934–940.
16. Solanki, J.; Fröhleke, N.; Böcker, J. Implementation of hybrid filter for 12-pulse thyristor rectifier supplying high-current variable-voltage DC load. *IEEE Trans. Ind. Electron.* **2015**, *62*, 4691–4701.
17. Aqueveque, P. E.; Wiechmann, E. P.; Burgos, R. P. On the efficiency and reliability of high-current rectifiers. In Proceedings of 2008 IEEE Power Electronics Specialists Conference, Rhodes, Greece, 15-19 June 2008, doi: 10.1109/PESC.2008.4592674.
18. Solanki, J.; Fröhleke, N.; Böcker, J.; Wallmeier, P. Analysis, design and control of 1MW, high power factor and high current rectifier system. In Proceedings of 2012 IEEE Energy Conversion Congress and Exposition (ECCE), Raleigh, NC, USA, 15-20 September 2012, doi: 10.1109/ECCE.2012.6342604.
19. Mohamadian, S.; Ghandehari, R.; Shoulaie, A. A comparative study of AC/DC converters used in high current applications. In Proceeding of 2011 2nd Power Electronics, Drive Systems and Technologies Conference, Tehran, Iran, 16-17 February 2011, doi: 10.1109/PEDSTC.2011.5742491.
20. Rodriguez, J.R.; Pontt, J.; Silva, C.; Wiechmann, E.P.; Hammond, P.W.; Santucci, F.W.; Alvarez, R.; Musalem, R.; Kouro, S.; Lezana, P. Large current rectifiers: State of the art and future trends. *IEEE Trans. Ind. Electron.* **2005**, *52*, 738–746.
21. Solanki, J.; Fröhleke, N.; Böcker, J.; Averberg, A.; Wallmeier, P. High-current variable-voltage rectifiers: state of the art topologies. *IET Power Electron.* **2015**, *8*, 1068–1080, doi: 10.1049/iet-pel.2014.0533.
22. PowerKraft^{TM} power supply solution for hydrogen production, KraftPowercon. Available online: https://kraftpowercon.com/ product/powerkraft (assesed on 30th Jan. 2022).
23. Maniscalco, P.S.; Scaini, V.; Veerkamp, W.E. Specifying DC chopper systems for electrochemical applications. *IEEE Trans. Ind. Appl.* **2001**, *37*, 941–948.
24. Scaini, V.; Ma, T. High-current DC choppers in the metals industry. *IEEE Ind. Appl. Mag.* **2002**, *8*, 26–33, doi: 10.1109/2943.985678.
25. Suh, Y.; Steimer, P. K. Application of IGCT in high-power rectifiers. *IEEE Trans. Ind. Appl.* **2009**, *45*, 1628–1636.
26. Koponen, J.; Ruuskanen, V.; Kosonen, A.; Niemelä, M.; Ahola, J. Effect of converter topology on the specific energy consumption of alkaline water electrolyzers. *IEEE Trans. Power Electron.* **2019**, *34*, 6171-6182, doi: 10.1109/TPEL.2018.2876636.
27. Solanki, J.; Fröhleke, N.; Böcker, J.; Wallmeier, P. Comparison of thyristor-rectifier with hybrid filter and chopper rectifier for high-power, high-current application. In Proceeding of PCIM Europe 2013, Nuremberg, Germany, 14-16 May 2013.
28. THYROBOX DC 3 industrial high-power dc power supply, AEG Power Solutions. Available online: https://www.aegps.com/en /products/dc-systems-industrial/thyrobox-dc-3-dc-3c/ (assessed on 30th Jan. 2022).
29. Liserre, M; Blaabjerg, F; Hansen, S. Design and control of an LCL-filter-based three-phase active rectifier. *IEEE Trans. Ind. Appl.* **2005**, *41*, 1281–1291.
30. Available online: https://nelhydrogen.com/resources/ (accessed on 23rd Nov. 2021).
31. IEC 60146-1-1, Semiconductor converters - general requirements and line commutated converters - part 1-1: specification of basic requirements.
32. IEC 61000-6-2, Electromagnetic compatibility (EMC) - part 6-2: generic standards - immunity standard for industrial environments.
33. IEC 61000-6-4, Electromagnetic compatibility (EMC) - part 6-4: generic standards - emission standard for equipment in industrial environments.
34. IEC 61000-3-6, Electromagnetic compatibility (EMC) – part 3-6: limits – assessment of emission limits for the connection of distorting installations to MV, HV and EHV power systems.
35. IEC 61000-3-7, Electromagnetic compatibility (EMC) – part 3-7: limits – assessment of emission limits for the connection of fluctuating installations to MV, HV and EHV power systems.
36. IEC 61000-6-13, Electromagnetic compatibility (EMC) - part 3-13: limits - assessment of emission limits for the connection of unbalanced installations to MV, HV and EHV power systems.
37. Efficient green hydrogen production with power electronics, Technology presentation, SEMIKRON Elektronik GmbH, Sept. 2021.
38. Nishimura, T.; Kakiki, H.; Kobayashi, T. High-power IGBT modules for industrial use, Fuji Electric Co., Ltd. Available online: https://www.fujielectric.com/company/tech/pdf/r52-2/03.pdf (assessed on 30th Jan. 2022).
39. Gennaro, F. Active front end converters for high power charging stations with high frequency SiC enabled operations. In Proceeding of 2020 ELEKTRO, Taormina, Italy, 25-28 May 2020, doi: 10.1109/ELEKTRO49696.2020.9130334.

40. Mao, S.; Wu, T.; Lu, X.; Popovic, J.; Ferreira, J.A. Three-phase active front-end rectifier efficiency improvement with silicon carbide power semiconductor devices. In Proceeding of 2016 IEEE Energy Conversion Congress and Exposition (ECCE), Milwaukee, WI, USA, 18-22 Sept. 2016, doi: 10.1109/ECCE.2016.7855515.
41. Kashihara, Y.; Nemoto, Y.; Qichen, W.; Fujita, S.; Yamada, R.; Okuma, Y. An isolated medium-voltage AC/DC power supply based on multil-cell converter topology. In Proceeding of 2017 IEEE Applied Power Electronics Conference and Exposition, Tampa, FL, USA, 26-30 March 2017, doi: 10.1109/APEC.2017.7931002.
42. Huber, J.E.; Kolar, J.W. Applicability of solid-state transformers in today's and future distribution grids. *IEEE Trans. Smart Grid* **2019**, *10*, 317–326, doi: 10.1109/TSG.2017.2738610.
43. Huber, J.E.; Kolar, J.W. Optimum number of cascaded cells for high-power medium-voltage ac–dc converters. *IEEE J. Emerg. Sel. Top. Power Electron.* **2017**, *5*, 213–232, doi: 10.1109/JESTPE.2016.2605702.
44. Cortes, P.; Huber, J; Silva, M.; Kolar, J.W. New modulation and control scheme for phase-modular isolated matrix-type three-phase AC/DC converter. In Proceeding of IECON 2013 - 39th Annual Conference of the IEEE Industrial Electronics Society, Vienna, Austria, 10-13 Nov. 2013, doi: 10.1109/IECON.2013.6699928.
45. Schrittwieser, L.; Cortés, P.; Fässler, L.; Bortis, D.; Kolar, J.W. Modulation and control of a three-phase phase-modular isolated matrix-type PFC rectifier. *IEEE Trans. Power Electron.* **2018**, *33*, 4703–4715, doi: 10.1109/TPEL.2017.2726342.
46. Rothmund, D.; Guillod, T.; Bortis, D.; Kolar, J.W. 99% efficient 10 kV SiC-based 7 kV/400 V dc transformer for future data centers. *IEEE J. Emerg. Sel. Top. Power Electron.* **2019**, *7*, 753–767, doi: 10.1109/JESTPE.2018.2886139.
47. Rothmund, D. 2018. 10 kV SiC-based medium-voltage solid-state transformer concepts for 400 V dc distribution systems. Ph.D. dissertation, ETH Zurich, Zurich, Switzerland.
48. Fang, F.; Li, Y.; Tian, H.; Li, Y.W. A carrier-based modulation strategy for modular isolated matrix rectifiers. *IEEE Trans. Ind. Appl.*, early access, doi: 10.1109/TIA.2021.3138035.
49. De Doncker, R. W., Divan, D. M., Kheraluwala, M. H. A three-phase soft-switched high-power-density DC/DC converter for high-power applications. *IEEE Trans. Ind. Appl.* **1991**, *27*, 63–73, doi: 10.1109/28.67533.
50. Yang, B.; Lee, F. C.; Zhang, A. J.; Huang, G. LLC resonant converter for front end DC/DC conversion. In Proceeding of 2002 IEEE 17th Annual IEEE Applied Power Electronics Conference and Exposition, Dallas, TX, USA, 10-14 March 2002, doi: 10.1109/APEC.2002.989382.